EDGE ARTICLE

Check for updates

Carbene derived diradicaloids – building blocks for singlet fission?†

Julian Messelberger,[a] Annette Grünwald,[a] Piermaria Pinter,[b] Max M. Hansmann [ID][c] and Dominik Munz [ID] *[a]

Organic singlet diradicaloids promise application in non-linear optics, electronic devices and singlet fission. The stabilization of carbon allotropes/cumulenes (C_1, C_2, C_4) by carbenes has been equally an area of high activity. Combining these fields, we showed recently that carbene scaffolds allow as well for the design of diradicaloids. Herein, we report a comprehensive computational investigation (CASSCF/NEVPT2; fractional occupation DFT) on the electronic properties of carbene–bridge–carbene type diradicaloids. We delineate how to adjust the properties of these ensembles through the choice of carbene and bridge and show that already a short C_2 bridge results in remarkable diradicaloid character. The choice of the carbene separately tunes the energies of the S_1 and T_1 excited states, whereas the bridge adjusts the overall energy level of the excited states. Accordingly, we develop guidelines on how to tailor the electronic properties of these molecules. Of particular note, fractional occupation DFT is an excellent tool to predict singlet–triplet gaps.

Introduction

The synthesis and spectroscopic scrutiny of organic diradicals is a vibrant area of research.[1–5] These molecules are suitable for organic field-effect transistors (OFETs),[6,7] non-linear optics,[8] two-photon absorption (TPA),[8] energy storage[9] and organic spintronics[10] due to their unique physico-chemical properties. Of particular importance, organic diradicals allow for the construction of solar cells based on singlet fission.[11–14] Singlet fission, *i.e.* the conversion of one excited singlet state to two triplet states, promises a breakthrough for a new generation of photovoltaics. While current materials are typically limited to a maximum of 33% (Shockley–Queisser limit),[15] singlet fission permits in principle quantum efficiencies of 200%.[16,17] One of the major limitations for singlet fission based light harvesting is the limited number and structural similarity of chromophores currently known to undergo this process.

It has consequently been emphasized that it is "essential that additional classes of efficient singlet fission chromophores be discovered".[18] One very well-known example for a Kekulé diradicaloid is Tschitschibabin's hydrocarbon (Fig. 1).[19] This molecule can be understood by two resonance structures, which correspond to the cumulenic closed-shell singlet state and the diradical open-shell state, which could be either an open-shell singlet or a triplet (Fig. 1).[20,21] The relative weights of these closed-shell and open-shell resonance structures are associated with the diradicaloid character of the molecule. Spectroscopic investigations of organic diradicals are unfortunately challenging due to their typically high reactivity. Therefore, much work has been devoted on taming these reactive compounds through the extension of the π-system,[22,23] introduction of stabilizing heteroatoms,[24–28] and/or the kinetic stabilization by steric bulk. We introduced carbenes as suitable building blocks for the isolation of carbene–bridge–carbene ensembles with very high diradicaloid character (Fig. 2).[29] The synthetic approach followed a straightforward and highly modular route, which allows for the combination of any stable free carbene with a large variety of different connecting bridges. Our synthetic efforts were inspired and guided by the fact that cyclic (alkyl)(amino) carbenes (CAACs)[30] stabilize organic radicals very well,[31–35] whereas N-heterocyclic carbene (NHC)[36] derived radicals[37,38] appear to be more reactive.

Further examples of cumulenes connected by two NHCs with saturated[39,40] and unsaturated[41] backbones were very recently reported. Equally, heterocyclic carbenes can stabilize cumulenes
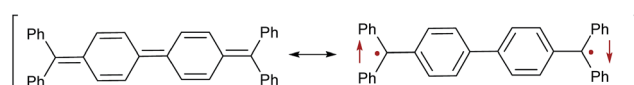
[a] Friedrich-Alexander Universität Erlangen-Nürnberg, Anorganische und Allgemeine Chemie, Egerlandstr. 1, 91058 Erlangen, Germany. E-mail: dominik.munz@fau.de

[b] Technische Universität Dresden, Physikalische Organische Chemie, Bergstr. 66, 01069 Dresden, Germany

[c] Georg-August Universität Göttingen, Institut für Organische und Biomolekulare Chemie, Tammannstraße 2, 37073 Göttingen, Germany

† Electronic supplementary information (ESI) available: Atomic coordinates, energies, delineation of the choice of the active space, FOD-plots, benchmark results, correlation plots, weight of configurations, molecular orbitals. See DOI: 10.1039/c8sc01999a
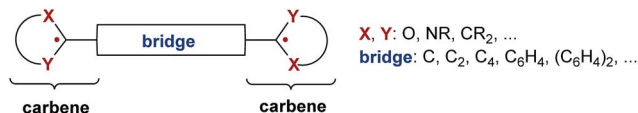
Fig. 1 Closed-shell singlet (left) as well as open-shell singlet (right) resonance structures of Tschitschibabin's diradicaloid.

Fig. 2 Modular synthesis of carbene derived diradicaloids and cumulenes.

and carbon allotropes,[42,43] which show unique optoelectronic properties.[44–48] We conclude therefore that carbenes are very likely to find many more applications in these areas. Key for the design of singlet or triplet diradicaloids is their electronic structure, which is most prominently reflected by their degree of diradicaloid character (*i.e.*, population of the lowest unoccupied molecular orbital LUMO).[49] Computational approaches offer here a convenient method to design such molecules.[50–55]

Herein, we report a detailed and comprehensive investigation using high-level CASSCF/NEVPT2 calculations on the (di)radical properties of carbene functionalized extended π-systems. We elucidate the influence of the carbene end groups and put them into perspective to other well-known diradicaloids and polyaromatic hydrocarbons (PAHs). We will quantify the effects of the cumulenic bridge and of the aromaticity. In particular, we describe which carbene leads to high diradical character. Eventually, we derive guidelines for tailoring the electronic properties of these diradicaloids for singlet fission in solar cells or two-photon absorption.

Results and discussion

Seven well-studied singlet diradicaloids were chosen as references (Fig. 3). Tschitschibabin's diradicaloid hydrocarbon (**1**) is related to Thiele's quinoid hydrocarbon (**2**), which was reported to be considerably more stable.[56] Tetracene (**3**) and pentacene (**4**), which have been extensively studied in the context of singlet fission, were picked as representative for fused π-systems.[57] Other prominent examples of this class include *e.g.* zethrenes,[58–60] phenalenyles,[61,62] quinodimethanes,[63–67] or diindeno fused π-systems.[68,69] The bisnitroxide (**5**),[70–74] bisoxoverdazyl (**6**),[75] and bisquinone (**7**)[76–79] were chosen as examples for heteroatom incorporation and supposedly very high diradical character.

The electronic and steric properties of singlet carbenes can be tuned in a straightforward fashion by adjacent π-donors,
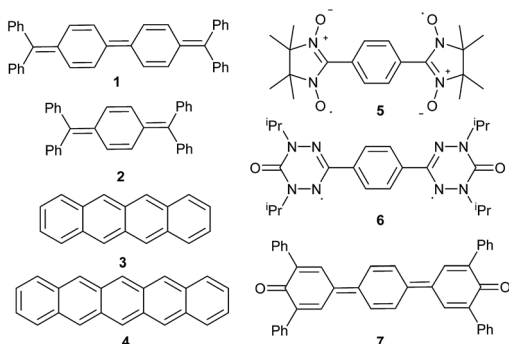
ring size, as well as aromaticity.[80–82] Cyclic (alkyl)(amino) carbenes (CAACs) with one nitrogen heteroatom adjacent to the carbene (Fig. 4; **8, 10–14**) allow for comparably efficient electron delocalization from the π-system of a bridge through their π-acceptor capabilities.

These derivatives were chosen in order to study the influence of the conjugated bridge, because most (**10**,[83] **11**,[42,43] **13**,[29] **14** [29]) are isolable. Additionally, we included the very recently synthesized NHC congener **9**.[41] Olefin substituents as modeled in **15** and **16** (*i.e.*, alkylidenes or dialkylcarbenes) and cyclic vinyl ether substituents (*i.e.*, Fischer carbenes) **17** should lead to even stronger electron delocalization. On the contrary, bisheteroatom substitution should give rise to electron richer derivatives (**18, 19**). The compounds **20–23** feature moderate to comparably strong aromatic character of the respective free carbenes. The attachment of mesoionic carbenes (**22**) and carbenes with significant carbodicarbene character (respectively bent allenes, **24**)[84–88] with significant population of the carbene's π-orbital gives access to very electron rich ensembles. Note that the bentallene **24** shows only very weak aromatic character as evidenced by the experimentally observed pyramidalization of the nitrogen atoms.[89]

Computational description of singlet diradicaloids[90]

The computational modeling of compounds with singlet-diradicaloid character is not a straightforward task. Although

Fig. 3 Isolated and herein studied molecular scaffolds with singlet diradicaloid character.
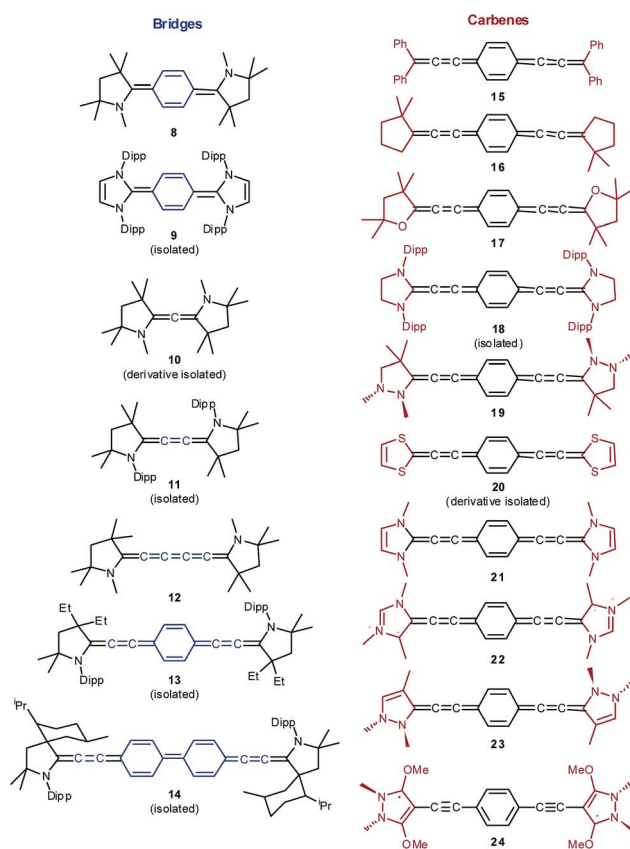

Fig. 4 Isolated and proposed carbene stabilized Kekulé diradicaloids studied herein. Structures **19**, **23** and **24** show pyramidalized amino groups.

unrestricted DFT is in principle capable of describing such systems using the broken-symmetry formalism,[91–94] the multireference singlet state is not well modeled for small singlet–triplet gaps. Spin decontamination procedures have been proposed to address the shortcomings – however, they also do not always lead to results in agreement with the experiment.[95–98] Indeed, we observed for the bisCAAC cumulenes that the description using DFT strongly underestimated the stability of the closed-shell singlet state and hence was not an appropriate method to predict the absorption spectra.[29] Multireference methods like the complete active space – self consistent field method (CASSCF)[99] are suitable for properly treating such systems.[100–105] Unfortunately, CASSCF is not a "black-box" procedure like DFT and the selection, *i.e.* quality, of the active orbitals typically determines the outcome of the calculation. The application of computational investigations using this and related methods remain therefore even for organic singlet diradicaloids comparably scarce,[50–52,55,103,106–117] whereas unrestricted DFT calculations are still much more commonly applied.[118–127]

A common descriptor of diradicaloid character are the diradical indices y_0 and y_1. They correspond to the natural orbital occupation number (NOON) of the lowest unoccupied natural orbital (LUNO) and LUNO+1, respectively, and are of course connected with the overall bond order.[128] A population of $y_0 = 1$ and $y_1 = 0$ signifies a diradical, whereas $y_0 = 1$ and $y_1 = 1$ describes a tetraradical. Non-linear optical properties like two-photon absorption are related with the second-order hyperpolarizability.[129–131] This property has been theoretically as well as experimentally shown to be enhanced for systems with a moderate singlet diradical contribution of about 36% (*i.e.*, $y_0 = 0.36$). It has also been suggested that molecules with a diradicaloid character above $y_0 = 0.1$ are in principle candidates for singlet fission as long as y_1 is considerably smaller than y_0.[132–134] Molecules with comparably low to intermediate y_0 values are also here expected to show higher energy efficiency.[135] The values of y_0 and y_1 are of course good indicators for the excitation energies related with these orbitals. They are therefore directly connected with the energy matching conditions for singlet fission processes.[127] A related approach, which relies on the relative weight of the closed-shell ("20") and double-excited configurations ("02") in a "two electrons in two orbitals" CI calculation has been proposed by Neese.[92,136]

Singlet fission is believed to be only feasible if the energy of the first excited singlet state $E(S_1)$ exceeds twice the energy of the triplet state $E(T_1)$ (eqn (1)).

$$2E(T_1) \approx E(S_1) \text{ and/or } 2E(T_1) < E(S_1) \tag{1}$$

For practical applications, the energy of the S_1 and twice the T_1 states should be in the same order of magnitude and close or moderately higher than 2.0 eV. Furthermore, twice the energy of the excited triplet state should be smaller than the energy of the second excited triplet state in order to avoid recombination processes of triplet excitons (eqn (2)).

$$2E(T_1) < E(T_2) \tag{2}$$

However, note that these two requirements are obviously not necessarily sufficient for the observation of singlet fission. Additionally, intermolecular interactions for this bimolecular process (electronic coupling) as well as molecular vibrations, which are associated with relaxation processes (vibronic coupling) are important.[54] Evidently, the stability of the excited states and the extinction coefficient are as well significant for light harvesting purposes. Another (computational) interpretive tool for the estimation of diradicaloid character, which relies on the fractional occupation number weighted electron density (N^{FOD}), was recently introduced by Grimme.[137,138] Of particular interest, this method comes at an extremely low computational cost. It is based on smearing the molecule's electrons over the molecular orbitals using finite temperature DFT and is a measure of static electron correlation. Molecules with a delocalized FOD and a large N^{FOD} have multireference character.

Computational methods

All complete active-space self-consistent-field (CASSCF)[99] calculations were performed with ORCA 4.0.1 (ref. 139) using the def2-TZVPP[140] basis set. The resolution of identity approximation and the related basis sets for both Coulomb and HF exchange integrals were used (RI-JK).[141] Tighter than default convergence criteria were chosen (tightscf). The second order perturbation theory NEVPT2 was applied to account for the effects of dynamic electron correlation.[142] The reported diradical indices as well as molecular orbital plots relate to the singlet ground states for all molecules. Five roots each were calculated for the state averaged modeling of the absorption spectra for the singlet states and triplet states. For the state-averaged CASSCF(14,14) calculations, three roots were calculated for the triplet- and four roots for the singlet states. Calculations using different number of roots (*e.g.*, 5 or 10) showed only very small deviation for the transition to the S_1 state and reordering of the states after the NEVPT2 correction is unproblematic when calculating at least 5 roots. Reported energies relate accordingly to vertical excitation from the S_0 states. Note that the geometry optimization of the excited states at the CAS level of theory is computationally extremely demanding. The structural parameters ("reorganization energy") of the molecules change moderately upon excitation. Geometry optimizations of **13** in the triplet state, closed-shell singlet state as well as broken-symmetry open-shell singlet state (B3LYP/def2-SVP) afforded similar structural parameters. *E.g.*, the distortion of the two acetylene units differs between the calculations by only about 10°. See the ESI† for CASSCF energies of the DFT optimized open-shell singlet, closed-shell singlet as well as triplet state of **13**. Nevertheless, the calculated adiabatic singlet–triplet gap is 0.73 eV, while the vertical excitations $^1S \rightarrow {}^3T$ for the solid state structure and the B3LYP closed-shell optimized structure are 0.80 eV and 0.98 eV, respectively. The choice of the active space for each molecule is delineated in detail in the ESI.† For the effect of enlarging the active space from 2 electrons in 2 orbitals, see as well the ESI.† An evaluation of basis set effects (def2-SVP, def2-TZVP, def2-TZVPP, def2-TZVPD, ma-def2-TZVPP, def2-QZVPP, cc-pVTZ, aug-cc-pVTZ)

indicates smooth convergence toward the complete basis limit and that def2-TZVPP is of sufficient quality for predicting the energies of the S_1 and T_1 states with a deviation of 0.04 eV from the largest basis set (ESI†). Typically, all the π-orbitals of the conjugated system were included up to 14 electrons in 14 orbitals [CASSCF(14,14)]. The NEVPT2 calculation for pentacene (**4**) evolved to be very time consuming for CASSCF(14,14) – therefore, the given energies relate to CASSCF(12,12). The predicted absorption wavelengths (energies of S_1 states, respectively) show a root mean square deviation RMSD from the experimentally determined values of 0.19 eV (mean deviation: 0.15 eV), which we consider an excellent fit (ESI†). Time dependent DFT using the B3LYP/def2-TZVPP level of theory underestimates the energy level of the S_1 state of *e.g.* **14** even without truncation by more than 0.5 eV. The deviation for the T_1 states, which is mainly due to the constrained geometric parameters (*vide supra*), appears to be larger and the calculations seem to systematically overestimate the singlet–triplet gap by up to 0.3 eV. However, note that experimental energies have only been reported for tetracene and pentacene, whereas the expected error for molecules with smaller π-system like **13** is expected to be smaller (the RMSD value for these two T_1 states and the calculated adiabatic singlet–triplet gap of **13** amount to 0.28 eV). The SMD implicit solvation model was applied for benchmark studies with experimental reported absorption spectra and led to moderately improved results (RMSD for S_1 states: 0.18 eV).[143,144] Increasing solvent polarity leads for **13** to a moderately increased level of the T_1 state, whereas the effects on the S_1 state appear to not follow a straightforward trend (ESI†). The absorption wavelengths reported in the manuscript are not corrected for solvation effects for comparability.

The structural parameters of **1–7**, **11**, **13**, **14**, **18** were obtained by optimization of the hydrogen atom positions from their solid state structures (B3LYP/def2-SVP). The D3 dispersion correction[145] with Becke–Johnson damping[146] was applied. All diisopropylphenyl (Dipp) groups and the menthyl substituent of structure **14** were truncated by methyl substituents. The iso-propyl groups of **6** and the phenyl substituents of structure **7** were modeled by methyl groups. The structures of all the other molecules were optimized in the singlet state without symmetry or internal coordinate constrains and were verified as true minima by the absence of negative eigenvalues in the harmonic vibrational frequency analysis. The restricted formalism, which showed very good agreement with the solid state structures for the CAAC derived molecules,[29] was used. The fractional occupation number weighted electron density (FOD) analysis was carried out with the default values as implemented in ORCA (TPSS/def2-TZVP; 5000 K). Calculated structures and molecular orbitals were visualized with Chemcraft, Avogadro 1.1.1 [147] and IBOView.[148]

Comparison carbene *vs.* non-carbene derived diradicaloids

The analysis of the electronic structure of **13** suggests strong cumulenic character and reveals that the localization of the two radicals as shown in Fig. 1 is an oversimplification (Fig. 5).

The diradicaloid character is mainly associated with the two frontier orbitals, which extend over the whole π-system and show an occupation of 1.71 (highest occupied natural orbital, HONO) and 0.29 (lowest unoccupied natural orbital, LUNO), respectively. Note that the CAAC moieties show a strong contribution of their p_z orbitals as well as of the adjacent amine groups. The occupancies of the HONO−1 (1.89) as well as the LUNO+1 (0.12) point at moderate tetraradical contributions.

In sight of an ideal diradical index of $y_0 = 0.36$ for a large two-photon absorption cross section (*vide supra*), we conclude that **13** should be a very good candidate for two-photon absorption.[8,131] The vertical excitation to the S_1 state can be approximated with a double excitation (29%) from the HONO to the LUNO and smaller single excitations from the HONO and HONO−1 to the LUNO (18%) and LUNO+1 (16%), respectively. This transition is expected to have very low intensity ($f^{osc} \approx 0.0$). The excitation to the S_2 state, which is only slightly higher in energy, involves mainly excitation of one electron to the LUNO (44%) with strong intensity ($f^{osc} \approx 0.9$). Hence, **13** qualifies as a class III chromophore (*vide infra*).[11]

The energy level of the S_1 state shows an energy gap of 2.49 eV in relation to the S_0 state, which is reasonable for applications associated with singlet fission. The vertical energy gap to the triplet state T_1 is a bit too low (0.80), whereas the level of the T_2 state is sufficiently high in energy (2.90 eV). To put the carbene derived singlet diradicaloid into perspective with well-studied congeners, we compare the CAAC derived diradicaloid **13** with Tschitschibabin's (**1**) as well as Thiele's (**2**) hydrocarbons and tetracene (**3**) as well as pentacene (**4**). Table 1 shows the most significant parameters for an evaluation of the electronic character of these molecules. The calculated absorption bands agree very well with the experimental values (**1**: $^{exp}\lambda = 576$ nm;[149] **2**: "orange";[56] **3**: $^{exp}\lambda = 475$ nm,[150] **4**: $^{exp}\lambda = 578$ nm,[11,151] **13**: $^{exp}\lambda = 551$ nm [29]). The calculated energies of the excited T_1 states appear to be a bit too high in comparison to the experimental values (*e.g.*, **3**: $^{exp}E(S_1)$: 2.61 eV; $^{exp}E(T_1)$: 1.34 eV; **4**: $^{exp}E(S_1)$: 2.13 eV; $^{exp}E(T_1)$: 0.95 eV),[11,151,152] which is mainly due to conformational changes associated with the transition to the T_1 states (ESI†). As evidenced by y_0 and N^{FOD}, the CAAC derived molecule shows significant diradicaloid character, which lies between Thiele's and Tschitschibabin's hydrocarbons and exceeds the one of tetracene. Note that the N^{FOD} values as well as plots (ESI†) indicate significant multireference character for all molecules. Experimentally, tetracene is well known to undergo singlet fission, although the process is slightly endergonic, *i.e.* $2E(T_1) > E(S_1)$ ("thermally activated singlet fission").[11] Tetracene
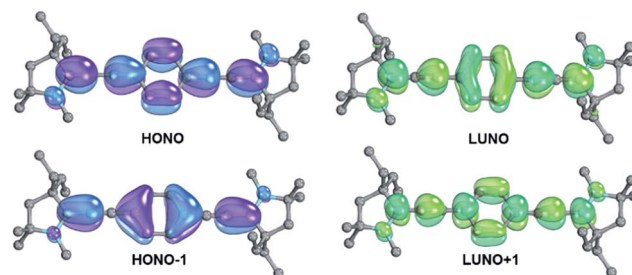

Fig. 5 Frontier orbitals of **13** as obtained from CASSCF(12,12) calculation.

Table 1 Diradical indices (y_0, y_1), N^{FOD}, vertical excitation energies E(S_1, T_1, T_2), absorption wavelengths and oscillation strength (f^{osc}) for $S_0 \rightarrow S_1$ transitions. Energies are given relative to the S_0 state and were obtained from CASSCF(12,12) calculations for **1**, **3**, **4** and **13** and from CASSCF(8,8) for **2**

Compound	1	2	3	4	13
y_0	0.47	0.19	0.18	0.19^a	0.29
y_1	0.12	0.08	0.08	0.09^a	0.12
N^{FOD}	1.36	0.60	0.52	0.89	0.85
E(S_1) in [eV]	2.13	2.41	2.46	2.07	2.49
E(T_1) in [eV]	0.41	1.59	1.65	1.23	0.80
E(T_2) in [eV]	2.79	3.90	2.90	2.50	2.90
Absorption $S_0 \rightarrow S_1$ (S_2) in [nm]	581 (339 S_2)	514	503	599	498 (444 S_2)
f^{osc} $S_0 \rightarrow S_1$ (S_2) in [nm]	0.0 (0.01)	0.6	0.1	0.13	0.0 (0.9)

^{a} The biradical indices relate to CASSCF(14,14), whereas the energies were only calculated with CASSCF(12,12) due to prohibitive computational demand for the NEVPT2 correction.

(note f^{osc} = 0.1) shows typically a very slow singlet-fission rate, which underlines the need for the development of novel materials.[153,154] Oxygen sensitive pentacene on the contrary shows experimentally slightly exoergic singlet fission.

Comparison of carbene derived diradicaloids

The CAAC (**8**) and NHC (**9**) derivatives of Thiele's hydrocarbon **2** (Table 2) are predicted to show a quite similar diradicaloid character (**2**: y_0 = 0.19; **8**: y_0 = 0.16; **9**: y_0 = 0.13). The energy levels of the excited T_1 states are moderately elevated [**2**: E(T_1) = 1.59 eV; **8**: E(T_1) = 1.70 eV; **9**: E(T_1) = 1.78 eV]. Interestingly, the diradical character of **2**, **8** and **9** is much smaller than the one of the nitroxide **5** or oxoverdazyl **6**. Both these compounds are almost perfect diradicals with energetically degenerate open-shell singlet and triplet ground states. The unpaired electrons are essentially localized on the heteroatoms with only very small contribution of the phenylene linkers (ESI†). The quinone congener **7** is predicted to show a diradical index, which is in between (y_0 = 0.32).

Table 3 collects all data for the carbene analogues of **13**. Olefin substitution by a "diphenylalkylidene" substituent (**15**) leads to quite low lying S_1 and T_1 states [E(S_1) = 1.59 eV; E(T_1) = 0.54 eV] and a high diradical index y_0 of 0.41 (Table 3). It is interesting to note that the "dialkylalkylidene" substituted diradicaloid **16** shows comparably elevated S_1 and T_1 states and reduced diradical character [E(S_1) = 2.56 eV, E(T_1) = 0.86 eV, y_0 = 0.30]. The very π-electron deficient "dialkylmethylidene"

group stabilizes accordingly the closed-shell cumulene. The high diradical character of **15** in comparison to **16** is – as also evidenced by electron delocalization of the relevant orbitals onto the phenyl rings – due to the radical-stabilizing influence of the aromatic phenyl substituents.

Dialkylcarbenes in their (excited) singlet state are of course more π-acidic than a Fischer carbene or CAAC with one π-electron donating oxo substituent or amine group, respectively. Decreasing the π-acceptor properties through introduction of an oxygen atom (**17**) reduces the diradical character as well as energy of the S_1 state very slightly [y_0 = 0.29, E(S_1) = 2.55 eV]. This trend holds when going to the amino derivative **13** [y_0 = 0.29, E(S_1) = 2.49 eV],[80,155,156] and the bisamino derivative **18** [y_0 = 0.26, E(S_1) = 2.35 eV]. The pyrazolidinylidene **19** [E(S_1) = 2.46 eV] shows similar properties. The experimental UV-Vis spectra reported for **13** and **18** agree well with the computational predictions with bands around 551 nm (**13**) and 595 nm (**18**). Both molecules appear to be electronically quite similar. We suggest therefore that the capability of saturated NHCs to stabilize organic radicals appears to be much stronger than commonly believed in the literature. Of particular interest is the comparison with the compounds **20–23**, where the free carbenes are considerably aromatic. These molecules show much lower energies for their S_1 states, which do not feature double excitation from the HONO. Especially the mesoionic carbene derivative **22** was predicted to be very reactive [E(S_1) = 0.96 eV; E(T_1) = 0.72 eV]. It does therefore not come as a surprise that it was recently experimentally found that saturated NHCs stabilize

Table 2 Diradical indices (y_0, y_1), N^{FOD}, vertical excitation energies E(S_1, T_1, T_2), calculated absorption wavelengths and oscillation strength (f^{osc}) for $S_0 \rightarrow S_1$ transitions. Energies are given relative to the S_0 state and were obtained from CASSCF(8,8) for **8** and CASSCF(12,12) for the other compounds

Compound	5	6	7	8	9
Substituent	Nitroxide	Oxo-verdazyl	Quinone	CAAC	NHC
y_0	1.0	1.0	0.32	0.16	0.13
y_1	0.16	0.14	0.09	0.09	0.09
N^{FOD}	2.14	2.10	1.34	0.47	0.69
E(S_1) in [eV]	2.30	3.09	2.19	2.74	2.46
E(T_1) in [eV]	0.0	0.0	0.75	1.70	1.78
E(T_2) in [eV]	2.2	2.97	2.90	3.51	2.79
Absorption $S_0 \rightarrow S_1$ (S_2) in [nm]	538	400	566	461	503
f^{osc} $S_0 \rightarrow S_1$	0.02	0.2	1.3	0.6	0.9

Table 3 Diradical indices (y_0, y_1), N^{FOD}, vertical excitation energies $E(S_1, T_1, T_2)$, calculated absorption wavelengths and oscillation strength (f^{osc}) for $S_0 \rightarrow S_1$ transitions. Energies are given relative to the S_0 state and were obtained from CASSCF(12,12) for **13–19**, **24** and CASSCF(14,14) for **20–23**

Compound Substituent	**15** Diphenyl-carbene	**16** Cyclopentylidene	**17** Cyclic Fischer carbene	**13** CAAC	**18** saNHC	**19** Pyrazolidin-ylidene	**20** TTF	**21** NHC	**22** MIC	**23** Pyrazolin-ylidene	**24** Bent allene
y_0	0.41	0.30	0.29	0.29	0.26	0.30	0.38	0.28	0.27	0.39	1
y_1	0.11	0.13	0.12	0.12	0.11	0.13	0.11	0.11	0.14	0.12	0.11
N^{FOD}	1.20	0.73	0.76	0.85	0.83	0.91	1.14	1.28	1.58	1.16	2.41
$E(S_1)$ in [eV]	1.59	2.56	2.55	2.49	2.35	2.46	2.07	1.67	0.96	1.89	2.37
$E(T_1)$ in [eV]	0.54	0.86	0.87	0.80	0.91	0.80	0.62	0.75	0.72	0.61	0
$E(T_2)$ in [eV]	2.64	2.90	2.90	2.90	2.97	2.83	2.55	2.19	0.84	2.31	2.30
Absorption $S_0 \rightarrow S_1$ (S_2, S_3) in [nm]	680	483 (276, S_3)	484 (288, S_3)	498 (444, S_2)	527	504 (433, S_2)	598	742	1297	625 (422, S_2)	522
f^{osc} $S_0 \rightarrow S_1$ (S_2, S_3)	1.0	0.0 (0.1, S_3)	0.0 (0.2, S_3)	0.0 (0.9, S_2)	1.1	0.0 (1.1, S_2)	1.1	1.2	0.2	0.0 (0.4, S_2)	0.01

radicals much better than aromatic NHCs.[38] Likewise, **21** is predicted to be much more reactive [$E(S_1) = 1.64$ eV] than **18**. The vertical singlet–triplet gap is also calculated to be comparably small [$E(T_1) = 0.75$ eV]. Eventually, we evaluated the electronic properties of **24**, which features two cyclic bent-allene molecules.[86,157–160] Bent allenes can be described as aliphatic carbene derivatives with a filled p_z orbital, i.e. they behave as π-donors.

Strikingly, perfect diradical character ($y_0 = 1$) and a very high N^{FOD} of 2.41 was calculated. The S_1 energy level of **24** [$E(S_1) = 2.37$ eV] is in the same order of magnitude as found for the other non-aromatic carbene derivatives **13–19**.

Fig. 6 illustrates the effect of all carbene substituents on the levels of the S_1 and T_1. Our calculations suggest accordingly that the population of the p_z orbital of the free aliphatic carbenes allows mainly for a tuning of the energy level of the T_1 state. On the contrary, aromaticity of the carbene has a very strong influence on the energy levels of mainly the S_1 states.

Comparison of bridges

Increasing the length of the linker leads to an increase of the diradicaloid character through insulation of the two formal radical centers. Especially the biphenylene bridged bisCAAC

Fig. 6 Energy levels of S_1 and twice the T_1 states for **13** and **16–24**. Derivatives of aliphatic carbenes are labeled with blue cycles, carbenes with aromatic character with red squares. Error bars relate to the root mean square deviation for the S_1 states from the experimentally available values.

compound **14** shows a very high diradical index of $y_0 = 0.78$ (Table 4), which is well reflected in the reduced electron density on the linker in the HONO and LUNO (Fig. 7). The singlet–triplet gap of this molecule becomes consequently very small [$E(T_1) = 0.21$ eV]. The calculated absorption spectrum is well in line with the experiment, where a band of small intensity was observed at 767 nm and a band of strong intensity at 653 nm.[161] The transition to S_2 ($f^{osc} = 1.0$) is mainly associated with a promotion of one electron from the HONO to the LUNO, whereas the S_1 state ($f^{osc} = 0.001$) corresponds to the double excitation as was obtained for **13** (vide supra). This chromophore qualifies accordingly also as a class III chromophore featuring a "doubly excited singlet state".[11] It is interesting to note that polyenes are typical class III chromophores, whereas aromatics usually belong to either class I or class II.[11]

The other compounds **8–12** on the contrary are class I chromophores, where the transition to the S_1 state is due to a single HONO–LUNO excitation. The CAAC stabilized carbon(0) (allene, respectively) **10** shows of course only negligible diradicaloid character. Surprisingly, already the C_2 derivative **11** has an energetically low-lying triplet state [$E(T_1) = 1.4$ eV] and is significantly diradicaloid ($y_0 = 0.22$, $N^{FOD} = 0.5$). Its diradical character is comparable to Thiele's hydrocarbon and tetracene (vide supra).

This unexpected diradical character has not been noticed in previous calculations,[43,162] but is equally reflected by the overall trend when going from **8** ($y_0 = 0.16$, $N^{FOD} = 0.5$) to "C_2-extended" **13** ($y_0 = 0.29$, $N^{FOD} = 0.8$). Equally, it explains perfectly why the NHC congener **21**, which is according to Tables 3 and 4 expected to show even larger diradicaloid character, could not be isolated in a previous synthetic study.[163] Note furthermore that **11**, which has been reported to be even stable at temperatures as high as 240 °C,[43] appears to be a good candidate for singlet fission [$E(S_1) = 2.88$ eV, $E(T_1) = 1.41$ eV] with a reasonable f^{osc} (0.63) for the relevant transition from the S_0 to the S_1 state.

Moving to carbene stabilized tetracarbon (**12**) or a phenylene (**8**) bridge reduces the energies of the S_1 states and elevates the energies of the T_1 states slightly [**8**: $E(S_1) = 2.74$ eV, $E(T_1) = 1.70$ eV; **12**: $E(S_1) = 2.82$ eV; $E(T_1) = 1.68$ eV]. The T_1 energy levels
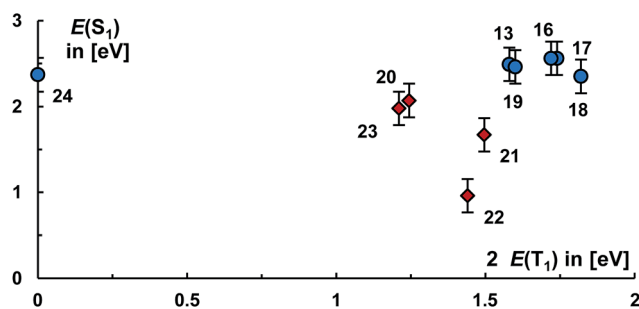
Table 4 Diradical indices (y_0, y_1), N^{FOD}, vertical excitation energies $E(S_1, T_1, T_2)$, calculated absorption wavelength and oscillation strength (f^{osc}) for $S_0 \rightarrow S_1$ transitions. Energies are given relative to the S_0 state and were obtained from CASSCF(4,4) for **10** and **11**, CASSCF(6,6) for **12**, CASSCF(8,8) for **8**, CASSCF(12,12) for **13** and CASSCF(14,14) for **14**

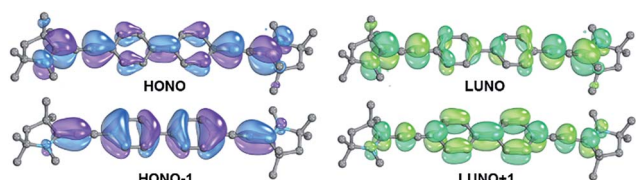| Compound	10	11	12	8	13	14
Bridge	C_1	C_2	C_4	C_6H_4	$CC-C_6H_4-CC$	$CC-C_6H_4-C_6H_4-CC$
y_0	0.07	0.22	0.16	0.16	0.29	0.78
y_1	0	0.04	0.07	0.09	0.12	0.11
N^{FOD}	0.06	0.50	0.47	0.47	0.85	1.43
$E(S_1)$ in [eV]	5.38	2.88	2.82	2.74	2.49	1.58
$E(T_1)$ in [eV]	4.27	1.41	1.68	1.70	0.80	0.21
$E(T_2)$ in [eV]	4.54	5.62	4.4	3.51	2.90	2.10
Absorption $S_0 \rightarrow S_1$ (S_2) in [nm]	231	430	442	461	498 (444)	784 (610)
f^{osc} $S_0 \rightarrow S_1$ (S_2)	0.0	0.6	0.0	0.6	0.0 (0.9)	0.0 (1.0)

Fig. 7 Frontier orbitals of **14** as obtained from CASSCF(14,14) calculation.

of **8, 11, 12**, are in an excellent range for practical applications as is found in tetracene.[153] Overall, we find therefore that enlarging the bridge affects both the energy levels of the S_1 and T_1 states. Fig. 8 puts the S_1 energy levels for the CAAC compounds **8, 10–14** into relation with the doubled value of the T_1 states. Importantly, the obtained fit $[E(S_1) = 0.89E(T_1) + 1.48$ eV] reveals that the S_1 as well as T_1 energy levels appear to be fairly linear dependent on the nature of the bridge. The choice of the bridge is accordingly an excellent tool for tailoring the overall level of the S_1 state.

Eventually, we would like to put all the molecules studied herein into perspective to each other. Fig. 9, left, relates the energies of the S_1 states with twice the energy of the T_1 states.

Evidently, carbenes allow for the synthesis of diradicaloids with a large electronic diversity, where most investigated structures satisfy the energy criteria for singlet fission. Overall, the calculated levels of the S_1 states range from 1.7 eV to 3.1 eV and the levels of the T_1 states from 0 eV to 1.8 eV. Plotting the

occupancies of the LUNO (y_0) as well as LUNO+1 (y_1) suggests likewise (Fig. 9, right) that many molecules studied herein qualify as very good candidates for singlet fission ($0.1 < y_0 < 0.5$; $y_1 \ll y_0$) and for two-photon absorption ($y_0 \approx 0.36$).

The molecules **8, 11, 12, 13, 16–21, 23** appear to be overall most promising for singlet fission, whereas **13, 15–23** should be good targets for two-photon absorption. Equally note that many of these molecules (**16–21, 23**) show comparably (in relation to their S_1 states and the values obtained for pentacene and especially tetracene) low lying T_1 states, which allows for considerably exoergic singlet fission. Of particular interest, we obtained an exponential relation $[\ln(N^{FOD}) = -0.81E(T_1) + 0.68]$ between the N^{FOD} and the energies of the excited T_1 states with a very good R^2 value of 96% (Fig. 10). The correlation of the N^{FOD}
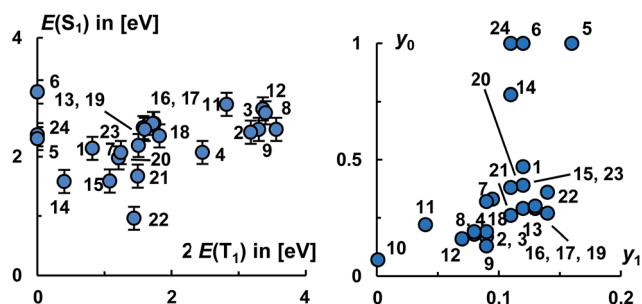

Fig. 9 Suitability of investigated diradicaloids for singlet fission according to energy matching condition of S_1 and T_1 states (left; **10** has been omitted for clarity) and the value of the diradical indices y_0 and y_1 (right). Error bars relate to the root mean square deviation for the S_1 states from the experimentally available values.
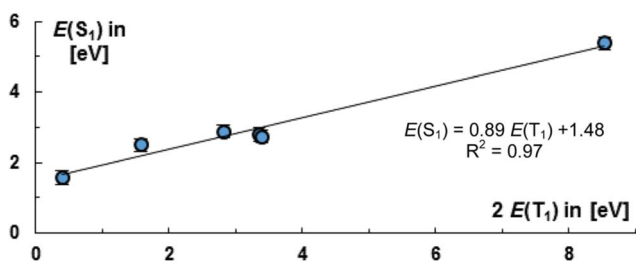

Fig. 8 Suitability of **8, 10–14** for singlet fission according to energy matching condition of the S_1 and T_1 states. Error bars relate to the root mean square deviation for the S_1 states from the experimentally available values.
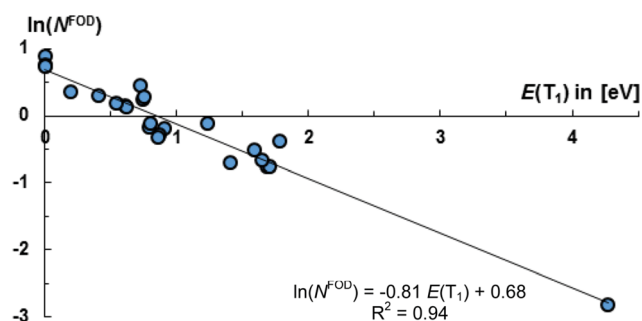

Fig. 10 The N^{FOD} is a good descriptor for the singlet–triplet gap.[164]

with the energies of the S_1 states, the population of the LUNO (y_0), or the correlation between y_0 and the energies of the T_1 states appears to be weaker (ESI†). We conclude therefore that the N^{FOD} is a reliable and time-efficient method for the estimation of the singlet–triplet gaps of these molecules.

Conclusions

Detailed CASSCF/NEVPT2 computations outline how to design carbene derived diradicaloids with tailored electronic properties for optoelectronic applications. Non-aromatic carbenes allow mainly for a tuning of the energies of the T_1 states. Aromaticity of the carbene groups has a very strong influence and reduces especially the energy level of the S_1 states. Overall, π-electron poor carbenes are predicted to lead to comparably low diradicaloid character, whereas π-electron rich C-donor ligands like bent allenes lead to "pristine" diradicals. The design of the bridge ("insulator") permits for an adjustment of the energy levels of both the first excited singlet and triplet states S_1 and T_1. Surprisingly, even very short bridges like carbene stabilized dicarbon (C_2) is predicted to show quite strong diradicaloid character. We observe that the capability of saturated NHCs to stabilize organic radicals appears to be stronger than commonly believed in the literature.

The fractional occupation number weighted electron density (N^{FOD}) is correlated with the energy levels of the T_1 state. Hence, it is an excellent predictive tools for the singlet–triplet gap.

Overall, the computations suggest that a considerable number of molecules studied herein are good candidates for application in singlet fission considering the energy matching criteria whereas some are suitable candidates for two-photon absorption. Our findings delineate how to obtain diradicaloids with desired electronic properties and give guidelines for merging carbene chemistry with singlet diradicaloid synthesis. We are convinced that diradicaloids derived from CAACs and NHCs with a saturated backbone are excellent candidates for optoelectronic applications and are therefore currently investigating their experimental behavior.

Conflicts of interest

There are no conflicts to declare.

Acknowledgements

Notes and references

1 M. Abe, *Chem. Rev.*, 2013, **113**, 7011–7088.
2 T. Y. Gopalakrishna, W. Zeng, X. Lu and J. Wu, *Chem. Commun.*, 2018, **54**, 2186–2199.
3 W. T. Borden, H. Iwamura and J. A. Berson, *Acc. Chem. Res.*, 1994, **27**, 109–116.
4 *Organic Redox Systems*, ed. T. Nishinaga, John Wiley & Sons, Inc, Hoboken, New Jersey, 2016.
5 Z. Zeng, X. Shi, C. Chi, J. T. Lopez Navarrete, J. Casado and J. Wu, *Chem. Soc. Rev.*, 2015, **44**, 6578–6596.
6 M. Chikamatsu, T. Mikami, J. Chisaka, Y. Yoshida, R. Azumi, K. Yase, A. Shimizu, T. Kubo, Y. Morita and K. Nakasuji, *Appl. Phys. Lett.*, 2007, **91**, 043506.
7 H. Koike, M. Chikamatsu, R. Azumi, J. y. Tsutsumi, K. Ogawa, W. Yamane, T. Nishiuchi, T. Kubo, T. Hasegawa and K. Kanai, *Adv. Funct. Mater.*, 2016, **26**, 277–283.
8 K. Kamada, K. Ohta, T. Kubo, A. Shimizu, Y. Morita, K. Nakasuji, R. Kishi, S. Ohta, S.-i. Furukawa, H. Takahashi and M. Nakano, *Angew. Chem., Int. Ed.*, 2007, **46**, 3544–3546.
9 Y. Morita, S. Nishida, T. Murata, M. Moriguchi, A. Ueda, M. Satoh, K. Arifuku, K. Sato and T. Takui, *Nat. Mater.*, 2011, **10**, 947–951.
10 V. A. Dediu, L. E. Hueso, I. Bergenti and C. Taliani, *Nat. Mater.*, 2009, **8**, 707–716.
11 M. B. Smith and J. Michl, *Chem. Rev.*, 2010, **110**, 6891–6936.
12 B. J. Walker, A. J. Musser, D. Beljonne and R. H. Friend, *Nat. Chem.*, 2013, **5**, 1019–1024.
13 J. Zirzlmeier, D. Lehnherr, P. B. Coto, E. T. Chernick, R. Casillas, B. S. Basel, M. Thoss, R. R. Tykwinski and D. M. Guldi, *Proc. Natl. Acad. Sci. U. S. A.*, 2015, **112**, 5325–5330.
14 N. J. Thompson, M. W. B. Wilson, D. N. Congreve, P. R. Brown, J. M. Scherer, T. S. Bischof, M. Wu, N. Geva, M. Welborn, T. V. Voorhis, V. Bulović, M. G. Bawendi and M. A. Baldo, *Nat. Mater.*, 2014, **13**, 1039–1043.
15 W. Shockley and H. J. Queisser, *J. Appl. Phys.*, 1961, **32**, 510–519.
16 D. N. Congreve, J. Lee, N. J. Thompson, E. Hontz, S. R. Yost, P. D. Reusswig, M. E. Bahlke, S. Reineke, T. Van Voorhis and M. A. Baldo, *Science*, 2013, **340**, 334–337.
17 O. E. Semonin, J. M. Luther, S. Choi, H.-Y. Chen, J. Gao, A. J. Nozik and M. C. Beard, *Science*, 2011, **334**, 1530–1533.
18 M. B. Smith and J. Michl, *Annu. Rev. Phys. Chem.*, 2013, **64**, 361–386.
19 A. E. Tschitschibabin, *Ber. Dtsch. Chem. Ges.*, 1907, **40**, 1810–1819.
20 L. K. Montgomery, J. C. Huffman, E. A. Jurczak and M. P. Grendze, *J. Am. Chem. Soc.*, 1986, **108**, 6004–6011.
21 P. Ravat and M. Baumgarten, *Phys. Chem. Chem. Phys.*, 2015, **17**, 983–991.
22 Z. Zeng, Y. M. Sung, N. Bao, D. Tan, R. Lee, J. L. Zafra, B. S. Lee, M. Ishida, J. Ding, J. T. López Navarrete, Y. Li, W. Zeng, D. Kim, K.-W. Huang, R. D. Webster, J. Casado and J. Wu, *J. Am. Chem. Soc.*, 2012, **134**, 14513–14525.
23 C. Jiang, Y. Bang, X. Wang, X. Lu, Z. Lim, H. Wei, S. El-Hankari, J. Wu and Z. Zeng, *Chem. Commun.*, 2018, **54**, 2389–2392.
24 Y. Su, X. Wang, X. Zheng, Z. Zhang, Y. Song, Y. Sui, Y. Li and X. Wang, *Angew. Chem., Int. Ed.*, 2014, **53**, 2857–2861.

25 Y. Su, X. Wang, L. Wang, Z. Zhang, X. Wang, Y. Song and P. P. Power, *Chem. Sci.*, 2016, **7**, 6514–6518.

26 S. Zheng, S. Barlow, C. Risko, T. L. Kinnibrugh, V. N. Khrustalev, S. C. Jones, M. Y. Antipin, N. M. Tucker, T. V. Timofeeva, V. Coropceanu, J.-L. Brédas and S. R. Marder, *J. Am. Chem. Soc.*, 2006, **128**, 1812–1817.

27 T. Li, G. Tan, D. Shao, J. Li, Z. Zhang, Y. Song, Y. Sui, S. Chen, Y. Fang and X. Wang, *J. Am. Chem. Soc.*, 2016, **138**, 10092–10095.

28 G. Tan and X. Wang, *Acc. Chem. Res.*, 2017, **50**, 1997–2006.

29 M. M. Hansmann, M. Melaimi, D. Munz and G. Bertrand, *J. Am. Chem. Soc.*, 2018, **140**, 2546–2554.

30 For the first report of a CAAC, see: (a) V. Lavallo, Y. Canac, C. Prasang, B. Donnadieu and G. Bertrand, *Angew. Chem., Int. Ed.*, 2005, **44**, 5705–5709. For reviews on CAACs, see: (b) M. Soleilhavoup and G. Bertrand, *Acc. Chem. Res.*, 2015, **48**, 256–266; (c) S. Roy, K. C. Mondal and H. W. Roesky, *Acc. Chem. Res.*, 2016, **49**, 357–369; (d) M. Melaimi, R. Jazzar, M. Soleilhavoup and G. Bertrand, *Angew. Chem., Int. Ed.*, 2017, **56**, 10046–10068; (e) U. S. D. Paul and U. Radius, *Eur. J. Inorg. Chem.*, 2017, 3362–3375.

31 J. K. Mahoney, D. Martin, F. Thomas, C. E. Moore, A. L. Rheingold and G. Bertrand, *J. Am. Chem. Soc.*, 2015, **137**, 7519–7525.

32 J. K. Mahoney, D. Martin, C. E. Moore, A. L. Rheingold and G. Bertrand, *J. Am. Chem. Soc.*, 2013, **135**, 18766–18769.

33 D. Munz, J. Chu, M. Melaimi and G. Bertrand, *Angew. Chem., Int. Ed.*, 2016, **55**, 12886–12890.

34 D. Martin, M. Soleilhavoup and G. Bertrand, *Chem. Sci.*, 2011, **2**, 389–399.

35 M. M. Hansmann, M. Melaimi and G. Bertrand, *J. Am. Chem. Soc.*, 2018, **140**, 2206–2213.

36 For thematic issues and books on NHCs, see: (a) T. Rovis and S. P. Nolan, *Synlett*, 2013, **24**, 1188–1189; (b) A. J. Arduengo and G. Bertrand, *Chem. Rev.*, 2009, **109**, 3209–3210; (c) S. Diez Gonzalez, *N-Heterocyclic Carbenes: From Laboratory Curiosities to Efficient Synthetic Tools*, Royal Society of Chemistry, Cambridge, 2010; (d) S. P. Nolan, *N-Heterocyclic Carbenes: Effective Tools for Organometallic Synthesis*, Wiley-VCH, Weinheim, 2014.

37 R. Ghadwal, D. Rottschäfer, B. Neumann, H.-G. Stammler, M. van Gastel and D. Andrada, *Angew. Chem., Int. Ed.*, 2018, **130**, 4855–4859.

38 P. L. Arnold and S. T. Liddle, *Organometallics*, 2006, **25**, 1485–1491.

39 B. Barry, G. Soper, J. Hurmalainen, A. Mansikkamäki, K. N. Robertson, W. L. McClennan, A. J. Veinot, T. L. Roemmele, U. Werner-Zwanziger, R. T. Boeré, H. M. Tuononen, J. Clyburne and J. Masuda, *Angew. Chem., Int. Ed.*, 2018, **57**, 749–754.

40 R. S. Ghadwal, D. Rottschafer, B. Neumann, G. Stammler and D. M. Andrada, *Chem. Sci.*, 2018, **9**, 4970–4976.

41 D. Rottschäfer, N. K. T. Ho, B. Neumann, H. G. Stammler, M. v. Gastel, D. M. Andrada and R. S. Ghadwal, *Angew. Chem., Int. Ed.*, 2018, **57**, 5838–5842.

42 L. Jin, M. Melaimi, L. Liu and G. Bertrand, *Org. Chem. Front.*, 2014, **1**, 351–354.

43 Y. Li, K. C. Mondal, P. P. Samuel, H. Zhu, C. M. Orben, S. Panneerselvam, B. Dittrich, B. Schwederski, W. Kaim, T. Mondal, D. Koley and H. W. Roesky, *Angew. Chem., Int. Ed.*, 2014, **53**, 4168–4172.

44 *Acetylene Chemistry*, ed. P. J. S. François Diederich, P. J. Stang and R. R. Tykwinski, Wiley-VCH Verlag GmbH & Co. KGaA, 2005.

45 M. Kivala and F. Diederich, *Acc. Chem. Res.*, 2009, **42**, 235–248.

46 F. Diederich and M. Kivala, *Adv. Mater.*, 2010, **22**, 803–812.

47 P. Rivera-Fuentes and F. Diederich, *Angew. Chem., Int. Ed.*, 2012, **51**, 2818–2828.

48 D. Wendinger and R. R. Tykwinski, *Acc. Chem. Res.*, 2017, **50**, 1468–1479.

49 T. Chen, L. Zheng, J. Yuan, Z. An, R. Chen, Y. Tao, H. Li, X. Xie and W. Huang, *Sci. Rep.*, 2015, **5**, 10923.

50 T. Zeng, N. Ananth and R. Hoffmann, *J. Am. Chem. Soc.*, 2014, **136**, 12638–12647.

51 J. Wen, Z. Havlas and J. Michl, *J. Am. Chem. Soc.*, 2015, **137**, 165–172.

52 A. F. Schwerin, J. C. Johnson, M. B. Smith, P. Sreearunothai, D. Popović, J. Černý, Z. Havlas, I. Paci, A. Akdag, M. K. MacLeod, X. Chen, D. E. David, M. A. Ratner, J. R. Miller, A. J. Nozik and J. Michl, *J. Phys. Chem. A*, 2010, **114**, 1457–1473.

53 D. Lopez-Carballeira, D. Casanova and F. Ruiperez, *Phys. Chem. Chem. Phys.*, 2017, **19**, 30227–30238.

54 S. Ito, T. Nagami and M. Nakano, *J. Photochem. Photobiol., C*, 2018, **34**, 85–120.

55 S. Ito and M. Nakano, *J. Phys. Chem. C*, 2015, **119**, 148–157.

56 J. Thiele and H. Balhorn, *Ber. Dtsch. Chem. Ges.*, 1904, **37**, 1463–1470.

57 J. M. Robertson, V. C. Sinclair and J. Trotter, *Acta Crystallogr.*, 1961, **14**, 697–704.

58 F. Hinkel, J. Freudenberg and U. H. Bunz, *Angew. Chem., Int. Ed.*, 2016, **55**, 9830–9832.

59 W. Zeng, Z. Sun, T. S. Herng, T. P. Gonçalves, T. Y. Gopalakrishna, K.-W. Huang, J. Ding and J. Wu, *Angew. Chem., Int. Ed.*, 2016, **55**, 8615–8619.

60 S. Lukman, J. M. Richter, L. Yang, P. Hu, J. Wu, N. C. Greenham and A. J. Musser, *J. Am. Chem. Soc.*, 2017, **139**, 18376–18385.

61 W. Zeng, S. Lee, M. Son, M. Ishida, K. Furukawa, P. Hu, Z. Sun, D. Kim and J. Wu, *Chem. Sci.*, 2015, **6**, 2427–2433.

62 T. Kubo, *Chem. Rec.*, 2015, **15**, 218–232.

63 K. Ohashi, T. Kubo, T. Masui, K. Yamamoto, K. Nakasuji, T. Takui, Y. Kai and I. Murata, *J. Am. Chem. Soc.*, 1998, **120**, 2018–2027.

64 D. Xia, A. Keerthi, C. An and M. Baumgarten, *Org. Chem. Front.*, 2017, **4**, 18–21.

65 J. Casado, *Top. Curr. Chem.*, 2017, **375**, 73.

66 H. Isobe, Y. Takano, Y. Kitagawa, T. Kawakami, S. Yamanaka, K. Yamaguchi and K. N. Houk, *J. Phys. Chem. A*, 2003, **107**, 682–694.

67 J. L. Segura and N. Martín, *Chem. Rev.*, 1999, **99**, 3199–3246.

68 J. Ma, J. Liu, M. Baumgarten, Y. Fu, Y.-Z. Tan, K. S. Schellhammer, F. Ortmann, G. Cuniberti,

H. Komber, R. Berger, K. Müllen and X. Feng, *Angew. Chem., Int. Ed.*, 2017, **56**, 3280–3284.

69 G. E. Rudebusch, J. L. Zafra, K. Jorner, K. Fukuda, J. L. Marshall, I. Arrechea-Marcos, G. L. Espejo, R. Ponce Ortiz, C. J. Gómez-García, L. N. Zakharov, M. Nakano, H. Ottosson, J. Casado and M. M. Haley, *Nat. Chem.*, 2016, **8**, 753–759.

70 A. Caneschi, P. Chiesi, L. David, F. Ferraro, D. Gatteschi and R. Sessoli, *Inorg. Chem.*, 1993, **32**, 1445–1453.

71 P. Ravat, Y. Ito, E. Gorelik, V. Enkelmann and M. Baumgarten, *Org. Lett.*, 2013, **15**, 4280–4283.

72 C. Train, L. Norel and M. Baumgarten, *Coord. Chem. Rev.*, 2009, **253**, 2342–2351.

73 L. Catala, J. Le Moigne, N. Kyritsakas, P. Rey, J. J. Novoa and P. Turek, *Chem.–Eur. J.*, 2001, **7**, 2466–2480.

74 S. Tolstikov, E. Tretyakov, S. Fokin, E. Suturina, G. Romanenko, A. Bogomyakov, D. Stass, A. Maryasov, M. Fedin, N. Gritsan and V. Ovcharenko, *Chem.–Eur. J.*, 2014, **20**, 2793–2803.

75 J. B. Gilroy, S. D. J. McKinnon, P. Kennepohl, M. S. Zsombor, M. J. Ferguson, L. K. Thompson and R. G. Hicks, *J. Org. Chem.*, 2007, **72**, 8062–8069.

76 J. Zhou and A. Rieker, *J. Chem. Soc., Perkin Trans. 2*, 1997, 931–938.

77 R. West, J. A. Jorgenson, K. L. Stearley and J. C. Calabrese, *J. Chem. Soc., Chem. Commun.*, 1991, 1234–1235.

78 D. Schmidt, M. Son, J. M. Lim, M.-J. Lin, I. Krummenacher, H. Braunschweig, D. Kim and F. Würthner, *Angew. Chem., Int. Ed.*, 2015, **54**, 13980–13984.

79 S. Lee, F. Miao, H. Phan, T. S. Herng, J. Ding, J. Wu and D. Kim, *ChemPhysChem*, 2017, **18**, 591–595.

80 O. Back, M. Henry-Ellinger, C. D. Martin, D. Martin and G. Bertrand, *Angew. Chem., Int. Ed.*, 2013, **52**, 2939–2943.

81 K. Verlinden, H. Buhl, W. Frank and C. Ganter, *Eur. J. Inorg. Chem.*, 2015, 2416–2425.

82 D. Munz, *Organometallics*, 2018, **37**, 275–289.

83 For the report of the benzannulated congener, see: W. Grahn, H.-H. Johannes, J. Rheinheimer, B. Knieriem and E.-U. Würthwein, *Liebigs Ann.*, 1995, **6**, 1003–1009.

84 W. C. Chen, J. S. Shen, T. Jurca, C. J. Peng, Y. H. Lin, Y. P. Wang, W. C. Shih, G. P. Yap and T. G. Ong, *Angew. Chem., Int. Ed.*, 2015, **54**, 15207–15212.

85 W.-C. Chen, Y.-C. Hsu, C.-Y. Lee, G. P. A. Yap and T.-G. Ong, *Organometallics*, 2013, **32**, 2435–2442.

86 C. A. Dyker, V. Lavallo, B. Donnadieu and G. Bertrand, *Angew. Chem., Int. Ed.*, 2008, **47**, 3206–3209.

87 H. Schmidbaur and A. Schier, *Angew. Chem., Int. Ed.*, 2013, **52**, 176–186.

88 R. Tonner, F. Öxler, B. Neumüller, W. Petz and G. Frenking, *Angew. Chem., Int. Ed.*, 2006, **45**, 8038–8042.

89 H. V. Huynh, in *The Organometallic Chemistry of N-heterocyclic Carbenes*, John Wiley & Sons, Ltd, 2017, pp. 293–329.

90 For a review on the computational modelling of singlet fission, see: D. Casanova, *Chem. Rev.*, 2018, DOI: 10.1021/acs.chemrev.7b00601.

91 J. Grafenstein, E. Kraka, M. Filatov and D. Cremer, *Int. J. Mol. Sci.*, 2002, **3**, 360–394.

92 F. Neese, *J. Phys. Chem. Solids*, 2004, **65**, 781–785.

93 R. Caballol, O. Castell, F. Illas, I. d. P. R. Moreira and J. P. Malrieu, *J. Phys. Chem. A*, 1997, **101**, 7860–7866.

94 E. R. Davidson and W. T. Borden, *J. Phys. Chem.*, 1983, **87**, 4783–4790.

95 N. Ferre, N. Guihery and J. P. Malrieu, *Phys. Chem. Chem. Phys.*, 2015, **17**, 14375–14382.

96 J. P. Malrieu and G. Trinquier, *J. Phys. Chem. A*, 2012, **116**, 8226–8237.

97 S. Yamanaka, T. Kawakami, H. Nagao and K. Yamaguchi, *Chem. Phys. Lett.*, 1994, **231**, 25–33.

98 L. Noodleman, *J. Chem. Phys.*, 1981, **74**, 5737–5743.

99 B. O. Roos, P. R. Taylor and P. E. M. Siegbahn, *Chem. Phys.*, 1980, **48**, 157–173.

100 J. Pittner, P. Nachtigall, P. Čársky and I. Hubač, *J. Phys. Chem. A*, 2001, **105**, 1354–1356.

101 X. Li and J. Paldus, *J. Chem. Phys.*, 2008, **129**, 054104.

102 E. R. Davidson and A. E. Clark, *Int. J. Quantum Chem.*, 2005, **103**, 1–9.

103 J. P. Malrieu, R. Caballol, C. J. Calzado, C. de Graaf and N. Guihéry, *Chem. Rev.*, 2014, **114**, 429–492.

104 D. Casanova and M. Head-Gordon, *Phys. Chem. Chem. Phys.*, 2009, **11**, 9779–9790.

105 S. J. Stoneburner, J. Shen, A. O. Ajala, P. Piecuch, D. G. Truhlar and L. Gagliardi, *J. Chem. Phys.*, 2017, **147**, 164120.

106 P. M. Zimmerman, F. Bell, D. Casanova and M. Head-Gordon, *J. Am. Chem. Soc.*, 2011, **133**, 19944–19952.

107 A. Das, T. Muller, F. Plasser and H. Lischka, *J. Phys. Chem. A*, 2016, **120**, 1625–1636.

108 M. R. Momeni, *J. Chem. Theory Comput.*, 2016, **12**, 5067–5075.

109 S. Radenković, S. Marković and V. Milenković, *Chem. Phys.*, 2012, **545**, 132–137.

110 H. K. Powell and W. T. Borden, *J. Org. Chem.*, 1995, **60**, 2654–2655.

111 C. M. Isborn, E. R. Davidson and B. H. Robinson, *J. Phys. Chem. A*, 2006, **110**, 7189–7196.

112 O. Kwon and G. Chung, *Bull. Korean Chem. Soc.*, 2008, **29**, 2140–2144.

113 V. Barone, I. Cacelli, P. Cimino, A. Ferretti, S. Monti and G. Prampolini, *J. Phys. Chem. A*, 2009, **113**, 15150–15155.

114 J. Hachmann, J. J. Dorando, M. Avilés and G. K.-L. Chan, *J. Chem. Phys.*, 2007, **127**, 134309.

115 Z. Qu, D. Zhang, C. Liu and Y. Jiang, *J. Phys. Chem. A*, 2009, **113**, 7909–7914.

116 M. Melle-Franco, *Chem. Commun.*, 2015, **51**, 5387–5390.

117 A. Das, T. Müller, F. Plasser, D. B. Krisiloff, E. A. Carter and H. Lischka, *J. Chem. Theory Comput.*, 2017, **13**, 2612–2622.

118 D. Peng, X. Hu, D. Devarajan, D. H. Ess, E. R. Johnson and W. Yang, *J. Chem. Phys.*, 2012, **137**, 114112.

119 D. H. Ess, E. R. Johnson, X. Hu and W. Yang, *J. Phys. Chem. A*, 2011, **115**, 76–83.

120 C. U. Ibeji and D. Ghosh, *Phys. Chem. Chem. Phys.*, 2015, **17**, 9849–9856.

121 M. Bendikov, H. M. Duong, K. Starkey, K. N. Houk, E. A. Carter and F. Wudl, *J. Am. Chem. Soc.*, 2004, **126**, 7416–7417.

122 H. F. Bettinger, *Pure Appl. Chem.*, 2010, **82**, 905–915.

123 D.-e. Jiang and S. Dai, *J. Phys. Chem. A*, 2008, **112**, 332–335.

124 R. Rakhi and C. H. Suresh, *Phys. Chem. Chem. Phys.*, 2016, **18**, 24631–24641.

125 Y. Yang, E. R. Davidson and W. Yang, *Proc. Natl. Acad. Sci. U. S. A.*, 2016, **113**, E5098–E5107.

126 D. H. Ess and T. C. Cook, *J. Phys. Chem. A*, 2012, **116**, 4922–4929.

127 I. Paci, J. C. Johnson, X. Chen, G. Rana, D. Popović, D. E. David, A. J. Nozik, M. A. Ratner and J. Michl, *J. Am. Chem. Soc.*, 2006, **128**, 16546–16553.

128 D. Doehnert and J. Koutecky, *J. Am. Chem. Soc.*, 1980, **102**, 1789–1796.

129 M. Nakano, H. Fukui, T. Minami, K. Yoneda, Y. Shigeta, R. Kishi, B. Champagne, E. Botek, T. Kubo, K. Ohta and K. Kamada, *Theor. Chem. Acc.*, 2011, **130**, 711–724.

130 K. Kamada, K. Ohta, A. Shimizu, T. Kubo, R. Kishi, H. Takahashi, E. Botek, B. Champagne and M. Nakano, *J. Phys. Chem. Lett.*, 2010, **1**, 937–940.

131 M. Nakano, R. Kishi, S. Ohta, H. Takahashi, T. Kubo, K. Kamada, K. Ohta, E. Botek and B. Champagne, *Phys. Rev. Lett.*, 2007, **99**, 033001.

132 T. Minami, S. Ito and M. Nakano, *J. Phys. Chem. Lett.*, 2013, **4**, 2133–2137.

133 S. Ito, T. Minami and M. Nakano, *J. Phys. Chem. C*, 2012, **116**, 19729–19736.

134 T. Minami and M. Nakano, *J. Phys. Chem. Lett.*, 2012, **3**, 145–150.

135 Note that the morphology is of course very important in the solid state.

136 D. Herebian, K. E. Wieghardt and F. Neese, *J. Am. Chem. Soc.*, 2003, **125**, 10997–11005.

137 C. A. Bauer, A. Hansen and S. Grimme, *Chem.–Eur. J.*, 2017, **23**, 6150–6164.

138 N. D. Mermin, *Phys. Rev.*, 1965, **137**, A1441–A1443.

139 F. Neese, *Wiley Interdiscip. Rev.: Comput. Mol. Sci.*, 2012, **2**, 73–78.

140 F. Weigend and R. Ahlrichs, *Phys. Chem. Chem. Phys.*, 2005, **7**, 3297–3305.

141 F. Weigend, *J. Comput. Chem.*, 2008, **29**, 167–175.

142 C. Angeli, R. Cimiraglia, S. Evangelisti, T. Leininger and J. P. Malrieu, *J. Chem. Phys.*, 2001, **114**, 10252–10264.

143 A. V. Marenich, C. J. Cramer and D. G. Truhlar, *J. Phys. Chem. B*, 2009, **113**, 6378–6396.

144 C. J. Cramer and D. G. Truhlar, *Acc. Chem. Res.*, 2008, **41**, 760–768.

145 S. Grimme, J. Antony, S. Ehrlich and H. Krieg, *J. Chem. Phys.*, 2010, **132**, 154104.

146 S. Grimme, S. Ehrlich and L. Goerigk, *J. Comput. Chem.*, 2011, **32**, 1456–1465.

147 M. D. Hanwell, D. E. Curtis, D. C. Lonie, T. Vandermeersch, E. Zurek and G. R. Hutchison, *J. Cheminf.*, 2012, **4**, 1–17.

148 G. Knizia, *J. Chem. Theory Comput.*, 2013, **9**, 4834–4843.

149 J. Bourdon and M. Calvin, *J. Org. Chem.*, 1957, **22**, 101–116.

150 T. Okamoto, T. Suzuki, H. Tanaka, D. Hashizume and Y. Matsuo, *Chem.–Asian J.*, 2012, **7**, 105–111.

151 C. Hellner, L. Lindqvist and P. C. Roberge, *J. Chem. Soc., Faraday Trans. 2*, 1972, **68**, 1928–1937.

152 J. J. Burdett, A. M. Müller, D. Gosztola and C. J. Bardeen, *J. Chem. Phys.*, 2010, **133**, 144506.

153 A. B. Pun, S. N. Sanders, E. Kumarasamy, M. Y. Sfeir, D. N. Congreve and L. M. Campos, *Adv. Mater.*, 2017, **29**, 1701416.

154 H. L. Stern, A. Cheminal, S. R. Yost, K. Broch, S. L. Bayliss, K. Chen, M. Tabachnyk, K. Thorley, N. Greenham, J. M. Hodgkiss, J. Anthony, M. Head-Gordon, A. J. Musser, A. Rao and R. H. Friend, *Nat. Chem.*, 2017, **9**, 1205–1212.

155 S. V. C. Vummaleti, D. J. Nelson, A. Poater, A. Gomez-Suarez, D. B. Cordes, A. M. Z. Slawin, S. P. Nolan and L. Cavallo, *Chem. Sci.*, 2015, **6**, 1895–1904.

156 A. Liske, K. Verlinden, H. Buhl, K. Schaper and C. Ganter, *Organometallics*, 2013, **32**, 5269–5272.

157 V. Lavallo, C. A. Dyker, B. Donnadieu and G. Bertrand, *Angew. Chem., Int. Ed.*, 2009, **48**, 1540–1542.

158 I. Fernández, C. A. Dyker, A. DeHope, B. Donnadieu, G. Frenking and G. Bertrand, *J. Am. Chem. Soc.*, 2009, **131**, 11875–11881.

159 M. M. Hanninen, A. Peuronen and H. M. Tuononen, *Chem.–Eur. J.*, 2009, **15**, 7287–7291.

160 M. Christl and B. Engels, *Angew. Chem., Int. Ed.*, 2009, **48**, 1538–1539.

161 Note that the experimental UV-Vis spectrum relates to a mixture of *E* and *Z* isomers.

162 J. L. Dutton and D. J. D. Wilson, *Angew. Chem., Int. Ed.*, 2012, **51**, 1477–1480.

163 D. C. Georgiou, B. D. Stringer, C. F. Hogan, P. J. Barnard, D. J. D. Wilson, N. Holzmann, G. Frenking and J. L. Dutton, *Chem.–Eur. J.*, 2015, **21**, 3377–3386.

164 Compounds 7, 9, 21, 22 (which have NOT been omitted from the fit) appear to be outliers. Exploratory calculations suggest that enlarging the active space beyond CASSCF(14,14) leads to a better fit for these compounds.